Nature Methods

Visualizing mechanical tension across membrane receptors with a fluorescent sensor

Daniel R. Stabley, Carol Jurchenko, Stephen S. Marshall, Khalid S. Salaita

Supplementary Figure 1	Fabrication of glass surface-functionalized force sensors
Supplementary Figure 2	Zero-force conformation of the sensor
Supplementary Figure 3	Zero-force conformation of the sensor at physiological conditions
Supplementary Figure 4	Theoretical plots of PEG_{24} and PEG_{75} extension and quenching efficiency as a function of applied force
Supplementary Figure 5	Specific EGF-EGFR interactions are required to activate the force sensor
Supplementary Figure 6	Force sensor response requires a specific ligand-receptor interaction
Supplementary Figure 7	Specific EGF-EGFR interactions are required to activate the force sensor: role of apposed ligand

Nature Methods: doi:10.1038/nmeth.1747

Supplementary Figure 8	Data analysis of force sensor response
Supplementary Figure 9	Cell binding does not induce clustering of sensor
Supplementary Figure 10	Binding of EGF antibody to EGF ligand does not trigger the sensor
Supplementary Figure 11	The activity of EGF ligand is independent of linker length
Supplementary Figure 12	Flow chart of data analysis for converting quenching efficiency to force maps
Supplementary Figure 13	Stability of the sensor as a function of time

Nature Methods: doi:10.1038/nmeth.1747

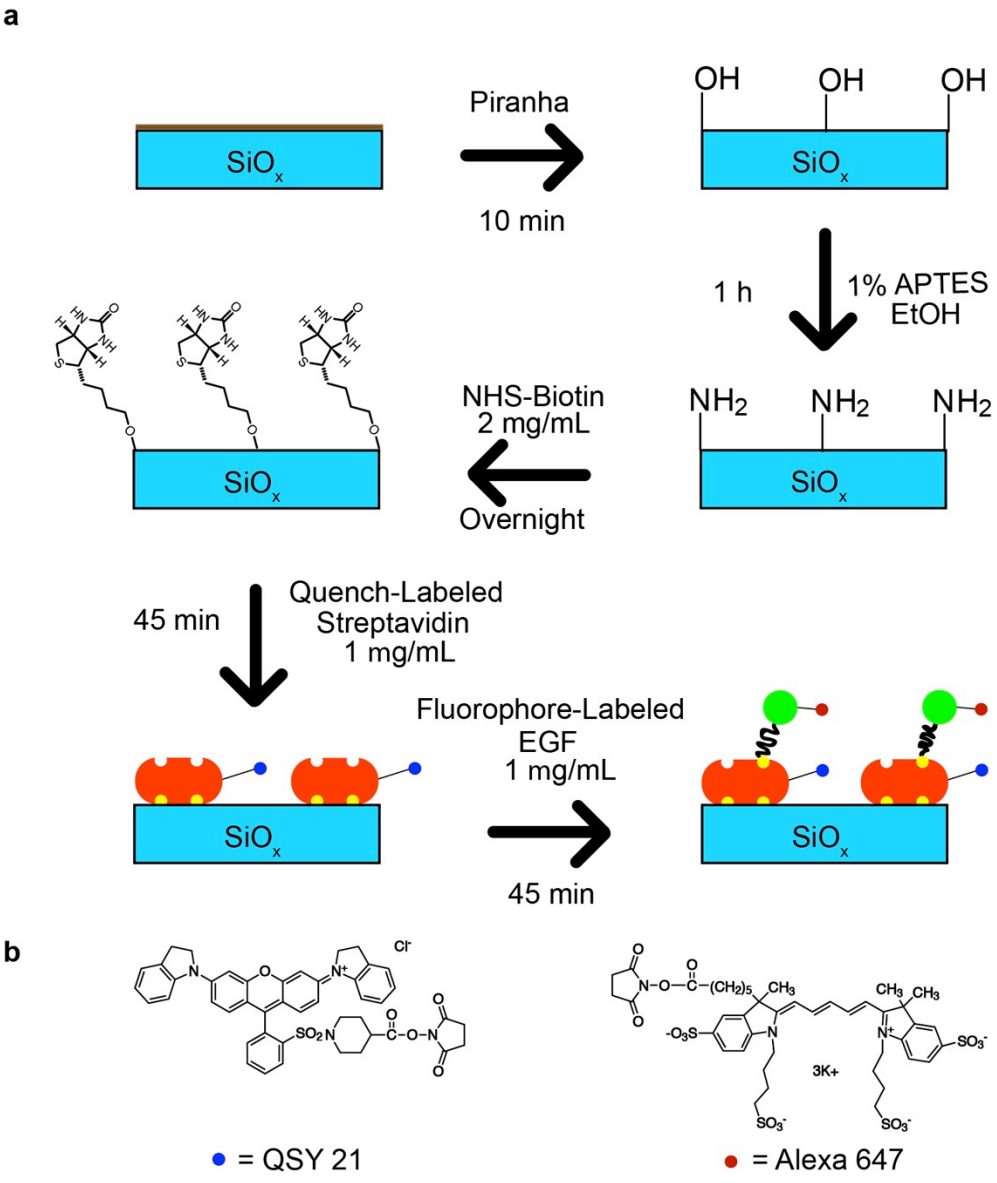

Supplementary Figure 1: Fabrication of glass surface-functionalized force sensors.

(**a**) Schematic describing the steps used to generate the force biosensors. See online methods section for detailed description. (**b**) Molecular structures of the reactive NHS esters of QSY 21 and Alexa 647.

Nature Methods: doi:10.1038/nmeth.1747

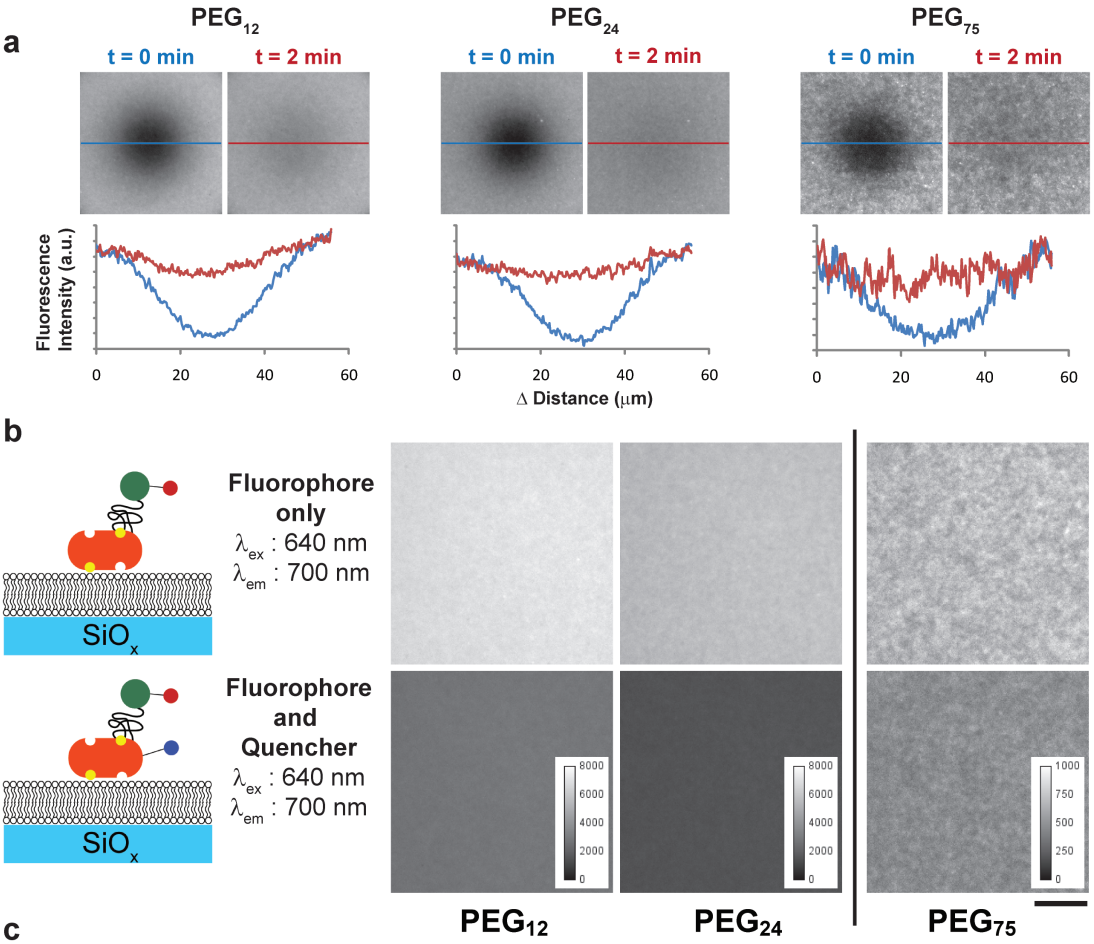

c

	PEG_{12}	PEG_{24}	PEG_{75}
Measured Quenching Efficiency	0.79 ± 0.01	0.85 ± 0.02	0.48 ± 0.03
Fluorophore-Quencher Distance (nm)	5.5 ± 0.1	5.2 ± 0.2	7.0 ± 0.2
Predicted Distance Based on Flory Model (nm)	4.6	5.4	7.7

Supplementary Figure 2: Zero-force conformation of the sensor.

(**a**) The force sensor surfaces are laterally fluid as indicated by FRAP (fluorescence recovery after photobleaching) experiments. Line plots show the fluorescence intensity

Nature Methods: doi:10.1038/nmeth.1747

immediately after photobleaching (blue) and the fluorescence intensity after 2 min of recovery time (red). (**b**) The resting state of EGF-PEG_{12}, EGF-PEG_{24}, and EGF-PEG_{75} sensors was determined by measuring the fluorescence intensity of surfaces containing the sensor in the absence (top row) and in the presence (bottom row) of the quencher. (**c**) The quenching efficiency for each surface was then calculated, and the experimental distance between chromophores in the resting state was determined and compared to the distance calculated from the Flory radius of each PEG polymer (see methods for calculation details). All measurements were taken in 1x PBS at RT. Error represents s.e.m. of three independent pairs of samples (n = 3) that were imaged at a minimum of five different locations each. Scale bar is 10 μm.

Nature Methods: doi:10.1038/nmeth.1747

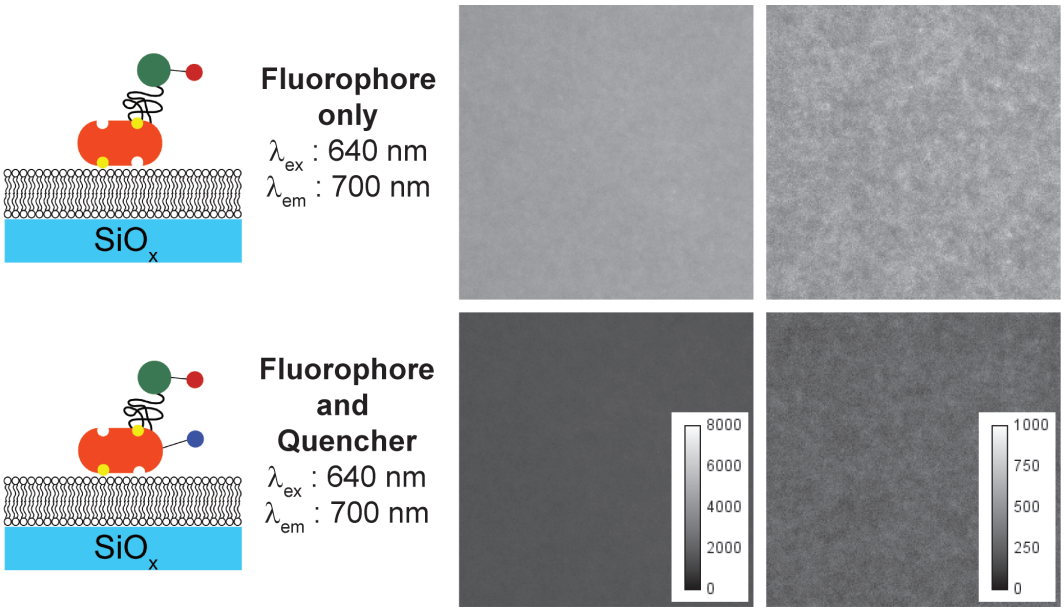

	PEG_{24}	PEG_{75}
Measured Quenching Efficiency	0.81 ± 0.03	0.58 ± 0.04
Fluorophore-Quencher Distance (nm)	5.4 ± 0.2	6.6 ± 0.3
Predicted Distance Based on Flory Model (nm)	5.4	7.7

Supplementary Figure 3: Zero-force conformation of the sensor at physiological conditions.

Representative fluorescence images of the EGF-PEG_{24} and EGF-PEG_{75} force sensor surfaces that were generated either with labeled or unlabeled streptavidin. The PEG sensor conformation was determined using equations 1 and 2 as described in Supplementary Fig. 2. The conformation of the sensor at 37 °C is similar to that shown previously for the sensor at 25 °C (Supplementary Fig. 2). Error represents the standard deviation of intensity measurements from ten different areas across two separate surfaces. Scale bar is 10 μm.

Nature Methods: doi:10.1038/nmeth.1747

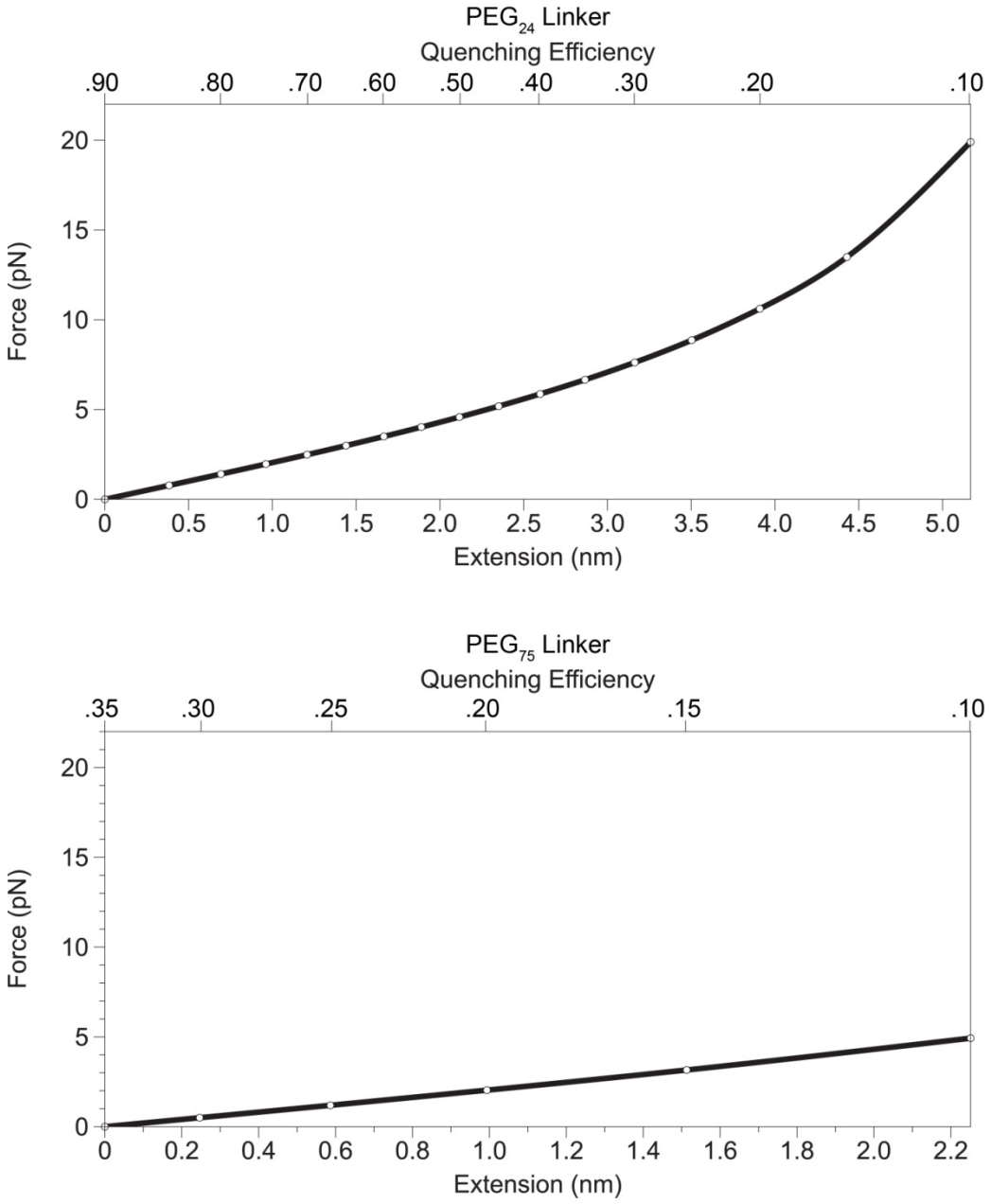

Supplementary Figure 4: Theoretical plots of PEG_{24} and PEG_{75} extension and quenching efficiency as a function of applied force.

The extended worm-like chain model (WLC) was used to generate a plot of the applied forces as a function of linker displacement, which is calculated from quenching efficiency (Eqn. 3-7). A range of quenching efficiencies from 10% to 90% was converted into PEG extension

Nature Methods: doi:10.1038/nmeth.1747

lengths using the FRET relation for the QSY 21 Alexa 647 quencher-fluorophore pair (Eqn. 4). The zero force resting state distance between the chromophores was calculated by subtracting the resting state of the polymer and the dimensions of the EGF and streptavidin proteins from the simulated distances. The resting state of the PEG_{24} linker was determined experimentally and corresponds to the polymer length at 90% quenching efficiency, while the PEG_{75} linker resting state was determined from the Flory model. The displacement from this resting state distance was then converted into a force using the extended WLC model. The PEG_{24} linker displays a wider dynamic range compared to PEG_{75} given the polymer conformations and the Förster radius of the QSY 21 and Alexa 647 pair.

Nature Methods: doi:10.1038/nmeth.1747

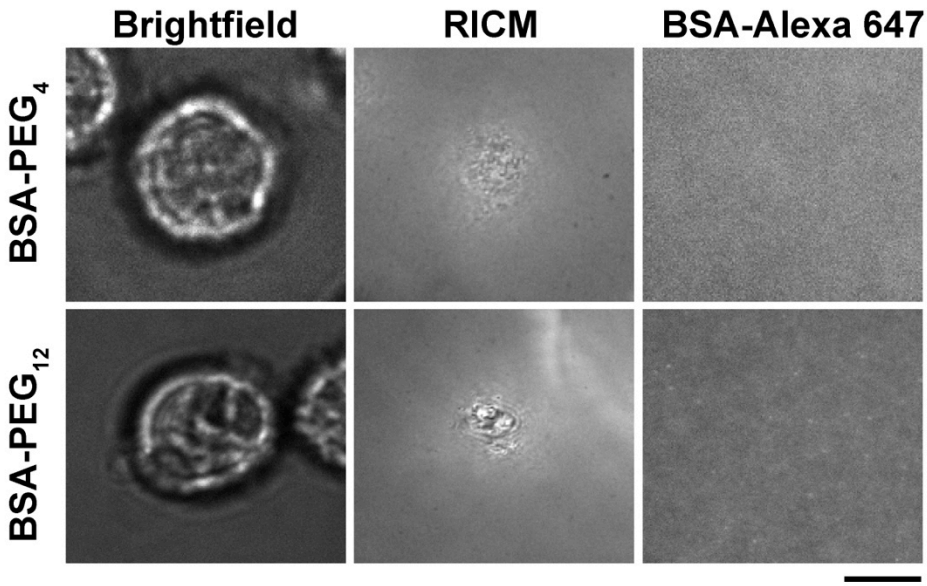

Supplementary Figure 5: Specific EGF-EGFR interactions are required to activate the force sensor.

Representative brightfield, RICM, and epifluorescence images of two cells on the indicated force sensor SLB (at t = 30 min). The fluorescence channel does not show any localized increases in signal, thus suggesting that a specific ligand-receptor interaction is necessary for force sensor activation. Scale bar is 10 μm.

Nature Methods: doi:10.1038/nmeth.1747

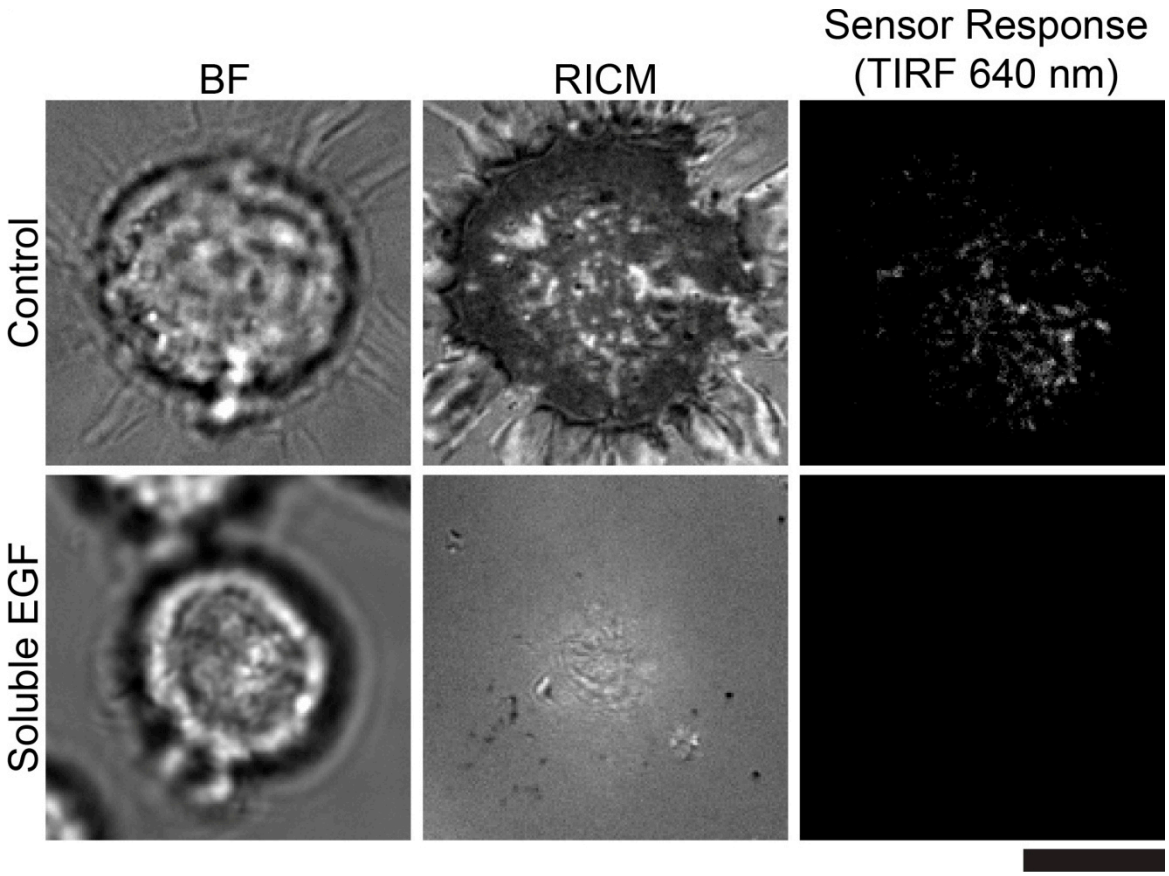

Supplementary Figure 6: Force Sensor response requires a specific ligand-receptor interaction.

Cells were plated on an EGF functionalized sensor surface either in the presence or absence of soluble EGF ligand (1.7 nM). Cells treated with soluble EGF exhibited poor adhesion to the surface and did not trigger a force sensor response, whereas control cells adhered strongly and generated the characteristic response. This indicates that the force sensor response is primarily mediated by the EGF-EGFR interaction. Scale bar is 10 μm.

Nature Methods: doi:10.1038/nmeth.1747

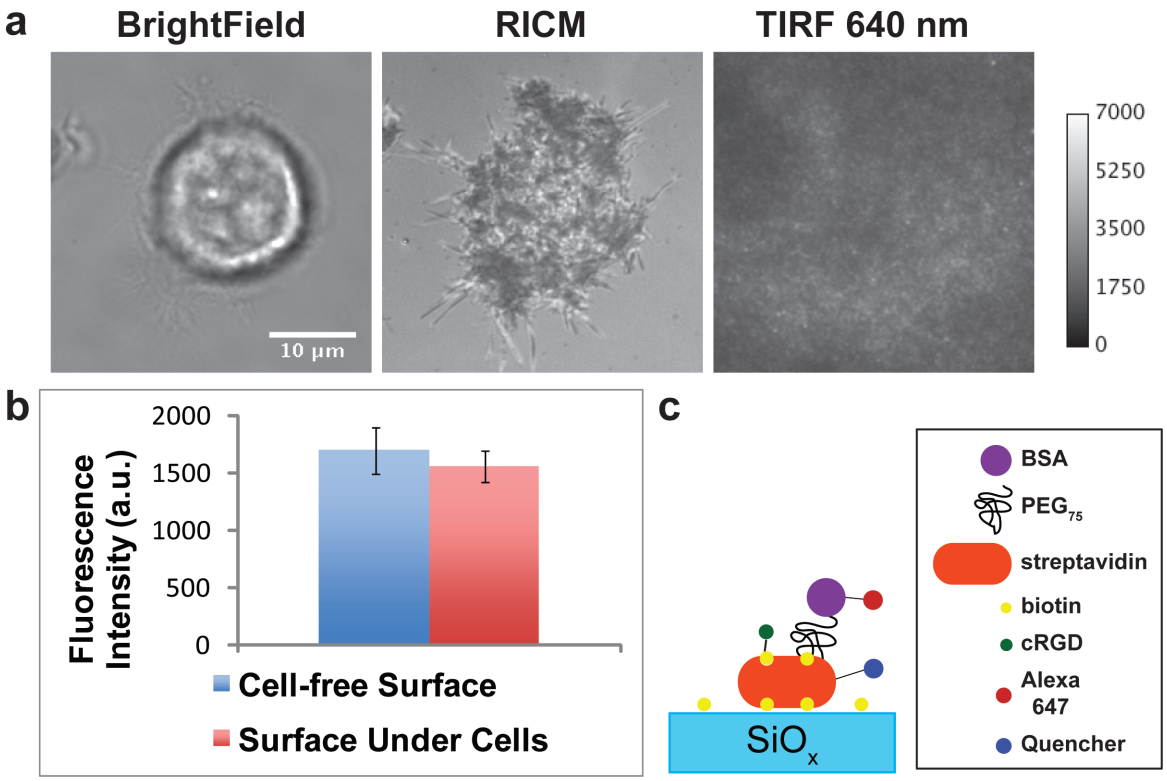

Supplementary Figure 7. Specific EGF-EGFR interactions are required to activate the force sensor: role of apposed ligand.

Brightfield, RICM, and TIRF (640 nm) images of a representative cell plated on a force sensor functionalized glass substrate. Cyclic RGD peptide (10 nM, Peptides Int'l) and BSA-PEG_{75}-Alexa 647 (15 nM) were co-adsorbed to the surface in order to provide two apposing ligands. The cRGD peptide engages integrins and enhances adhesion while the BSA provides a control force sensor ligand. The brightfield and RICM images (**a**) indicate that the cells are engaged to the surface. The TIRF image does not show any observable localized increases in signal, thus confirming that a specific ligand-receptor interaction is necessary for force probe response. (**b**) Comparison of the fluorescence intensities observed for the blank sensor surface with the area under the cells does not show a significant difference. Analysis represents the

Nature Methods: doi:10.1038/nmeth.1747

average of 10 cells. Error bars represent standard deviation. (**c**) Scheme depicting the BSA control force sensor.

Nature Methods: doi:10.1038/nmeth.1747

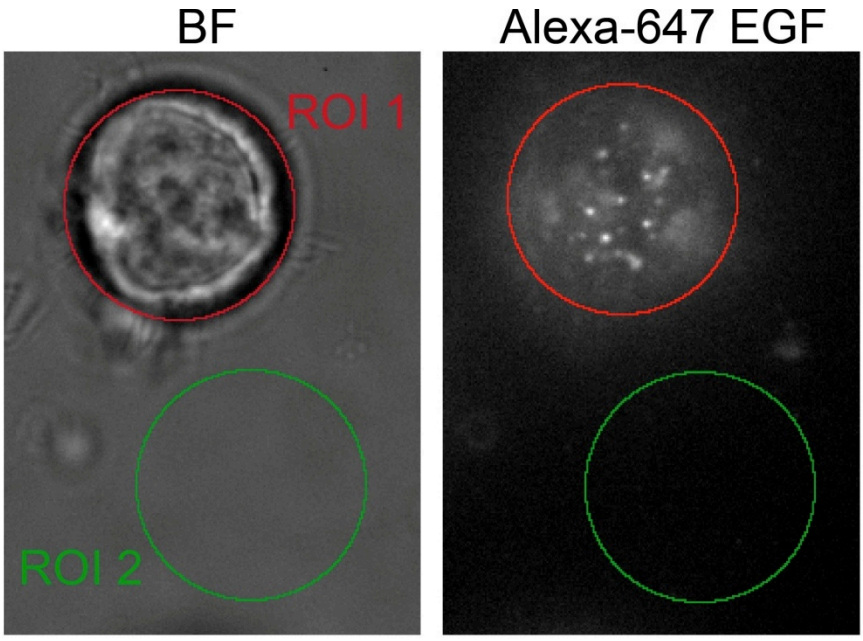

Supplementary Figure 8: Data analysis of force sensor response.

Using the brightfield images as a guide, each Alexa 647 EGF image is analyzed by placing a circular region of interest (ROI) over the area of a cell (ROI 1 (red) in images) as well as placing an ROI over an off-cell area (ROI 2 (green) in images). The average intensity of the fluorescence signal in each ROI is measured, and the mean intensity of ROI 1 is divided by the mean intensity of ROI 2. This is repeated for many cells, and the quotients are averaged into a mean, generating the normalized fluorescence increase values used in plots. The error reported is that of the measured quotients.

Nature Methods: doi:10.1038/nmeth.1747

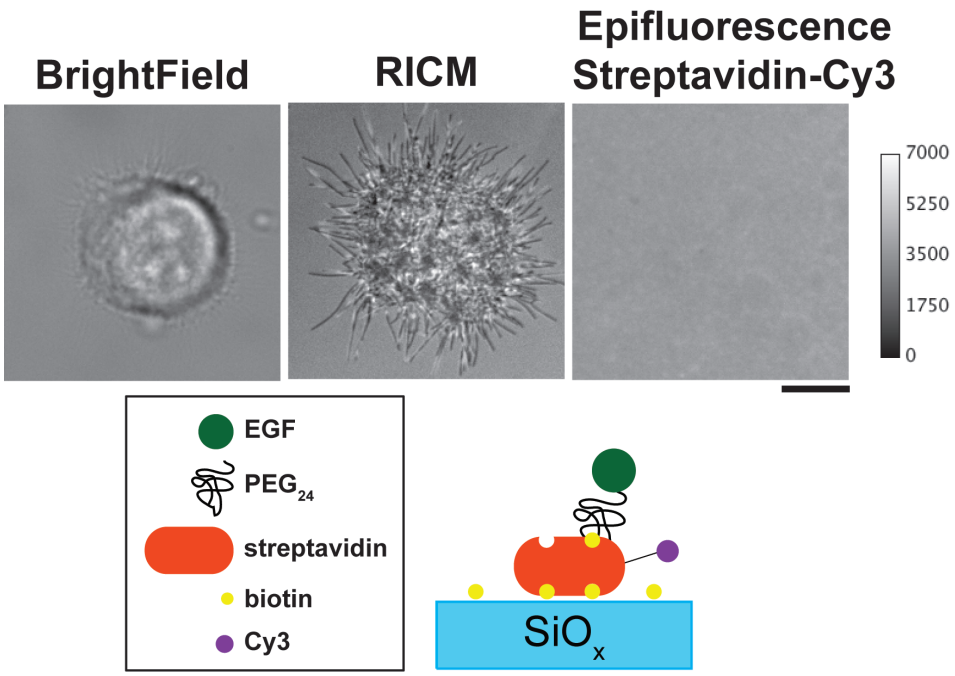

Supplementary Figure 9: Cell binding does not induce clustering of sensor.

HCC1134 cells were incubated for 30 min on surfaces functionalized with EGF-PEG_{24}-streptavidin-Cy3. Brightfield and RICM images show that the cell engaged the surface. Fluorescence images of the Cy3 channel do not show any observable clustering, which confirms that the streptavidin is immobile on the glass substrate. Scale bar is 10 µm.

Nature Methods: doi:10.1038/nmeth.1747

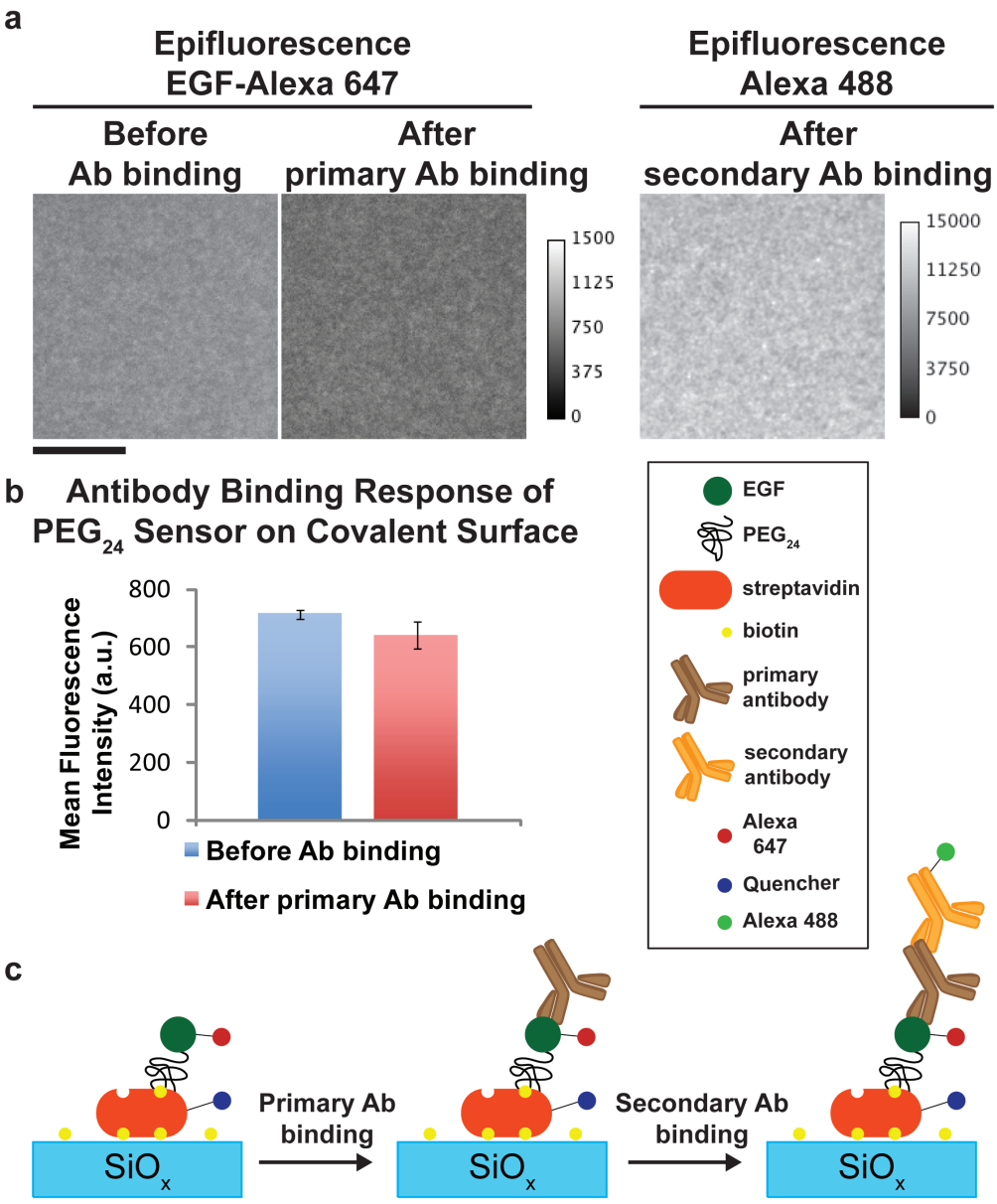

Supplementary Figure 10: Binding of EGF antibody to EGF ligand does not trigger the force sensor.

Surfaces were covalently functionalized with the force sensor containing EGF ligand as described previously. (**a**) Representative fluorescence images of the force sensor surface before and after binding of primary EGF antibody (5 μg ml^{-1}, R&D Systems). To confirm binding of antibody to the surface, the primary antibody surfaces were incubated with secondary IgG

Nature Methods: doi:10.1038/nmeth.1747

antibody-Alexa 488 (2.5 μg ml^{-1}, Invitrogen). (**b**) Bar graph showing the mean fluorescence intensity of force sensor surface before (blue) and after (red) addition of the primary antibody. Error represents the standard deviation of 10 different regions on each surface. (**c**) Scheme depicting the predicted antibody binding to the force sensor surface.

Nature Methods: doi:10.1038/nmeth.1747

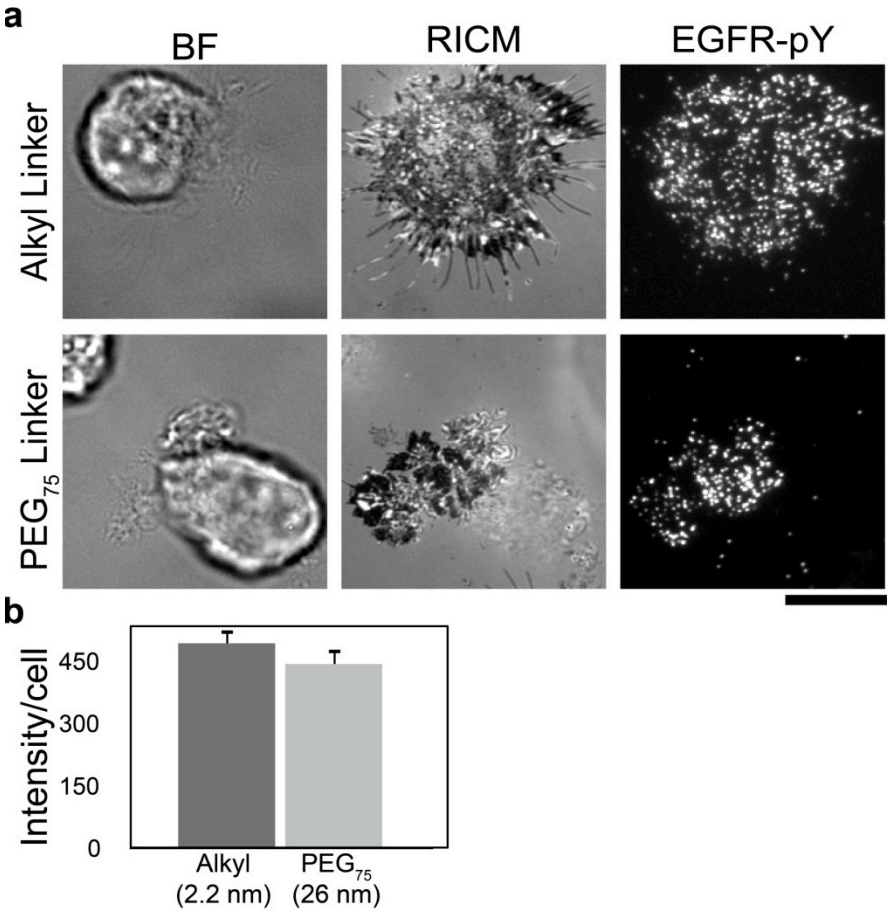

Supplementary Figure 11: The activity of EGF ligand is independent of linker length.

HCC1143 cells were serum starved for 18 h and plated onto sensor surfaces in supplemented RPMI media at 37 ˚C and incubated for approximately 30 min, after which cells were imaged live (see methods for imaging details). (**a**) Representative brightfield, images of two cells that were incubated onto the indicated sensor surface and then fixed and stained with anti-EGFR-pY 1068 antibody (Cell Signaling Technologies 3777s). Scale bar is 12μm. (**b**) Graph showing the average background-subtracted fluorescence intensity of cells immunostained for EGFR-pY 1068. Intensity indicates the level of receptor phosphorylation remains similar for both the alkyl and PEG_{75} linkers. Error bars represent the standard error of the mean (s.e.m.), alkyl, $n = 52$ cells; PEG_{75}, $n = 47$ cells.

Nature Methods: doi:10.1038/nmeth.1747

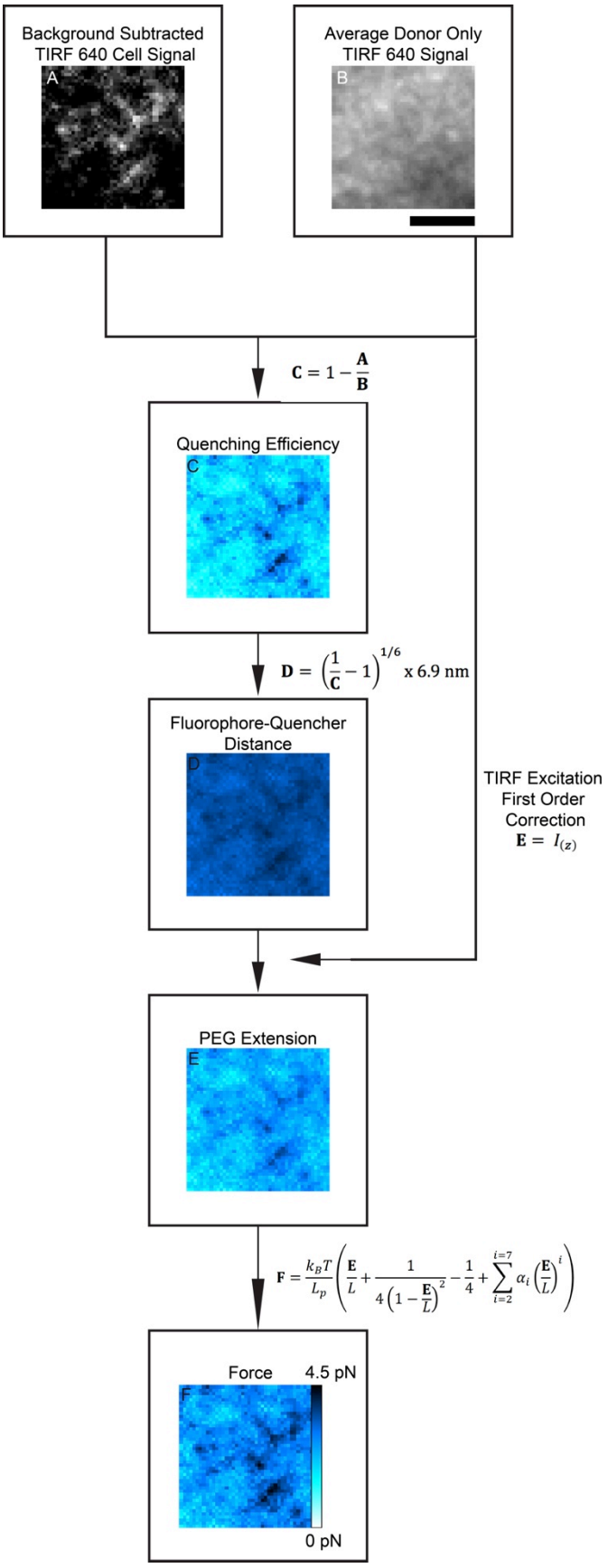

Nature Methods: doi:10.1038/nmeth.1747

Supplementary Figure 12: Flow chart of data analysis for converting quenching efficiency to force maps.

In order to quantify the forces detected by the sensor, a series of image operations were performed. First, the background subtracted TIRF 640 image (**A**) was divided by a composite donor only signal image (**B**) to generate a quenching efficiency image map (**C**). Note that (**B**) is an average of the signal over five regions of the donor only sample. The quenching efficiency map is then converted to a distance map (**D**) using the FRET relationship. This distance map is then used to perform a first order correction for TIRF excitation intensity falloff (see equations 5 and 6 in the online methods). After the dimensions of EGF, streptavidin, and the resting state of the polymer were subtracted out, the *z* extension of PEG was mapped (**E**). This extension image was then converted to force (**F**) using the extended WLC model (see online methods for more details). Note that the false-color intensity values represent an ensemble average force for each pixel, and that this is the lower bound of the applied force. Scale bar is 3.2 μm.

Nature Methods: doi:10.1038/nmeth.1747

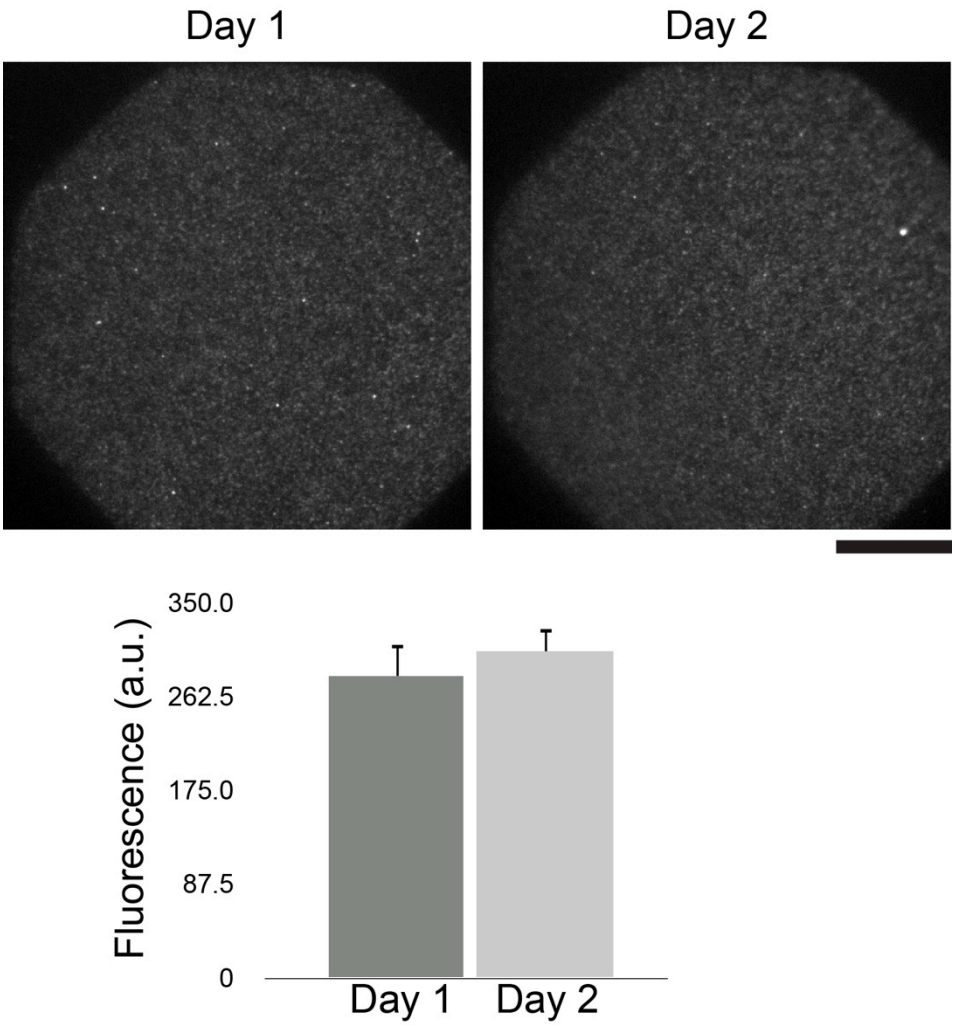

Supplementary Figure 13: Stability of the sensor as a function of time.

A sensor surface featuring Alexa 647 labeled EGF and QSY 21 labeled streptavidin was prepared and then imaged over the course of two days. There was no significant change in the fluorescence intensity after 24 hours, indicating that the quencher is stable over the span of experimental time scales. Scale bar is 20 μm, error represents the s.e.m. of three regions for each surface.

Nature Methods: doi:10.1038/nmeth.1747